

A STUDY OF REYNOLDS ANALOGY IN A HYPERSONIC BOUNDARY LAYER USING A NEW SKIN FRICTION GAUGE

G.M. KELLY, A. PAULL and J.M. SIMMONS

Department of Mechanical Engineering
 University of Queensland
 QLD 4072, AUSTRALIA

ABSTRACT

Skin friction measurements have been made in T4, the University of Queensland's hypervelocity free piston shock tunnel. The measurements were made on a flat plate in a compressible boundary layer. They are compared with heat transfer measurements made simultaneously. It is found that in the region where the boundary layer was laminar the results compare favourably with those predicted by Reynolds analogy. The onset of transition can be clearly seen with both types of instrumentation.

INTRODUCTION

Hypervelocity impulse facilities, such as free piston shock tunnels and expansion tubes, have an important role in the development of technologies for hypersonic flight. They are capable of generating the high-enthalpy flows associated with external aerodynamics of space planes at near orbital velocities and the internal aerodynamics of scramjet propulsion systems. Important model test parameters are drag and skin friction but their measurement is complicated greatly by the very short test times of impulse facilities. Skin friction measurement is complicated further by the fact that the wall pressure can be an order of magnitude greater than the wall stress generated by skin friction. Skin friction gauges for use in conventional shock tunnels have been reported. However, their ability to perform satisfactorily in the very short duration flows associated with free piston shock tunnels and expansion tubes does not appear to have demonstrated. This paper reports the development of a transducer capable of measuring skin friction with a rise time of about 20 μ s. Results prove the effectiveness of the concept when used to measure skin friction on a flat plate. Reynolds analogy is examined by comparing the output from heat transfer gauges and skin friction gauges. The onset of transition is also observed using both devices.

GAUGE DESIGN

The gauge design is shown schematically in Figure 1. It comprises a thin metal disk or thermal cover (10 mm diameter and 0.4 mm thick) mounted flush with the surface of the model and bonded to a stack of two piezoelectric transducer elements (each 7 x 7 mm and 1.5 mm thick). The material chosen for the elements was

the piezoceramic PZT-7A. Its rigidity and density were such that, for the configuration in Figure 1, gauge natural frequencies were above 300 kHz. In theory, the elements appropriately orientated and with electrodes on the appropriate surfaces, respond only to shear force generated by skin friction, but in practice there was a small pressure dependency (normal to the disk). For this reason the two-element gauge was designed, with one piezoceramic element inverted with respect to the other.

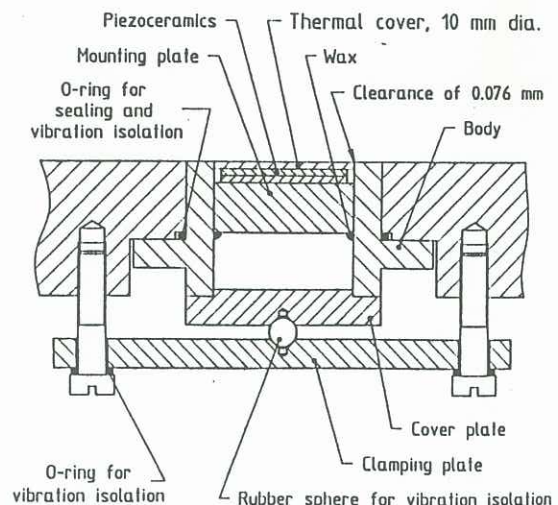


Figure 1 Schematic of skin friction gauge

One element provides an output e_1 proportional to the sum of the effects of skin friction τ and pressure p applied to the disk, and the other provides an output e_2 proportional to the differences [Equations (1) and (2) below].

A weighted summation of the two outputs therefore provides a direct measurement of shear stress.

$$e_1 = a_1\tau + b_1p \quad (1)$$

$$e_2 = a_2\tau - b_2p \quad (2)$$

A calibration procedure would involve using a known laminar boundary layer for a condition in the shock tunnel to determine constants a_1 and a_2 . To determine the pressure sensitivity it is necessary to apply a transient pressure, with $\tau = 0$, to the transducer to

determine the ratio of constants b_1/b_2 . Hence, an unknown shear stress τ can be determined from Equation (3) and simultaneous measurement of outputs e_1 and e_2 .

$$e_1 + (b_1/b_2)e_2 = [a_1 + (b_1/b_2)a_2]\tau \quad (3)$$

Piezoceramics exhibit a Curie temperature above which they begin to depolarise. To avoid this, the thickness of the thermal cover and its material were chosen to prevent unacceptable levels of conductive heat transfer from the hot test gas in the boundary layer. Several materials were evaluated. Invar was finally chosen because it has a very small coefficient of thermal expansion, thereby preventing the transducer elements from being strained due to thermal expansion of the disk.

The impulsive nature of the flow in free piston shock tunnels results in stress waves in the model, with the skin friction gauge exposed to a vibration-induced acceleration environment. To counteract this, rubber and felt vibration isolation was included in the design (Figure 1). The technique effectively lowered acceleration induced output from the gauge to a level that could be handled by filtering during signal processing.

The shear stress levels on the models were typically 200-1000 Pa, but for some of the flow conditions they were less than 100 Pa. Since the charge produced by the piezoceramic elements is small (of the order of 5 pC for some conditions), amplification of the signal was required. To minimise noise contamination, a charge amplifier was located as close as possible to the site of signal detection.

EXPERIMENT

To determine b_1/b_2 a small shock tube was used to apply a transient pressure and no shear stress to the skin friction gauge. The shear stress calibration yielding a_1 and a_2 was determined as mentioned previously using heat transfer measurements in a laminar boundary layer for a condition in the shock tunnel. Measurements were made of the heat transfer close to the site of the gauge and Reynolds analogy was then used to determine the skin friction.

Reynolds analogy can be stated as

$$\frac{C_H}{c_f} = \frac{1}{2} Pr^{-2/3} \quad (4)$$

where C_H is the coefficient of heat transfer and c_f the coefficient of skin friction. Pr is the Prandtl number. Using van Driest's determination of skin friction in a compressible, flat plate, laminar boundary layer (van Driest, 1952) and the assumption that the free stream conditions remain effectively constant, Reynolds analogy can be reduced to

$$\frac{q_w}{\tau} = \frac{-Pr^{-2/3} c_p [T_\infty (1 + r \frac{\gamma-1}{2} M_\infty^2) - T_w]}{U_\infty} \quad (5)$$

| | | |
|------------------|---|----------------------------------|
| Where T_∞ | = | free stream temperature, K |
| V_∞ | = | free stream velocity, m/s |
| M_∞ | = | free stream Mach Number |
| q | = | heat transfer, kW/m ² |
| τ | = | shear stress, kPa |
| c_p | = | specific heat |
| r | = | recovery factor |

Having determined the sensitivities of the gauges to shear stress from one test condition, these values were then used for the other three test conditions.

The flat plate model used was made of aluminium with a leading edge of steel (Figure 2). It was 600 mm in length and 228 mm in width. There were six skin friction gauges in the model, the first at a distance 145 mm from the leading edge and the others at 65 mm intervals downstream of it. At the site of every skin friction gauge a piezoelectric pressure transducer was positioned to one side and a thin film heat transfer gauge to the other. Their centres were set at the same distance from the leading edge. The sensing element on the skin friction gauge was a 10 mm diameter disk. The heat transfer gauge was 1.7 mm in diameter and the pressure tapings were 2 mm diameter. The available test time depended on the condition used, since for higher enthalpy conditions the signal was contaminated by noise earlier. For higher energy flows vibration travelled through the model earlier, reducing the available test time. The range of conditions used is listed in Table I. Condition 1 is that used for calibration purposes. Figure 3 shows the heat transfer distribution along the plate for the calibration test approximately 500 μ s after the start of the flow. This was the condition used to determine the shear sensitivities of the gauges. These sensitivities have then been used to determine shear stress profiles for the three other conditions.

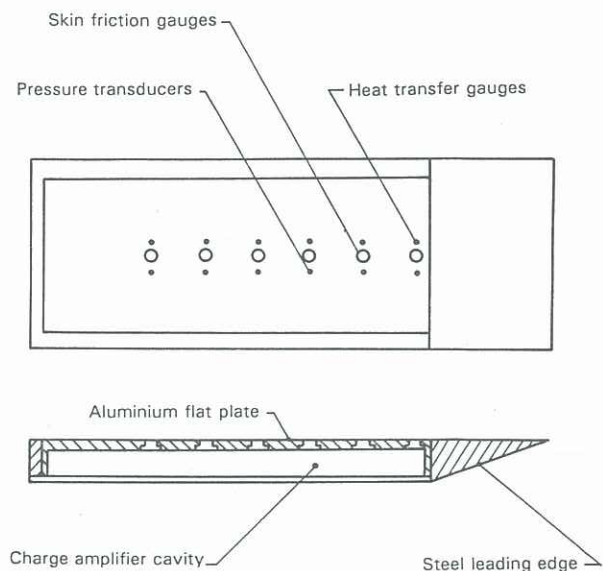


Figure 2 Schematic of flat plate model

RESULTS

Figure 4 shows the time-histories of heat transfer and the corresponding skin friction at position 1, 145 mm from the leading edge for condition 2. This condition was not used for calibration because transition occurs. The scale on the vertical axis is for both shear stress and heat transfer. The units are kPa and MW/m² respectively.

It can be seen from this trace that whilst the skin friction and heat transfer exhibit the same trends, rapid changes in the heat transfer due to transition tend to lag the skin friction. This is consistent with the development

of the thermal boundary layer. Basically the thermal profile develops more slowly than the velocity profile. Initially when the thermal boundary layer is thin the heat transfer rate is high and the responses of both the heat transfer gauge and the skin friction gauge are virtually simultaneous. Later in time, as the boundary layer grows, the heat transfer lags the skin friction. This effect becomes more marked downstream where the boundary layer is thicker. As the boundary layer thickens the heat transfer rate decreases.

Table I Four test conditions

| | 1 | 2 | 3 | 4 |
|----------------------------|-------|-------|-------|------|
| Stagnation enthalpy, MJ/kg | 4.58 | 7.27 | 7.59 | 9.06 |
| Stagnation temperature, K | 3522 | 4663 | 4921 | 5685 |
| Stagnation pressure, MPa | 11.16 | 9.375 | 20.04 | 51.3 |
| Temperature, K | 574.5 | 1129 | 1180 | 1297 |
| Pressure, kPa | 3.8 | 4.3 | 9.17 | 22.6 |
| Density, kg/m ³ | 0.023 | 0.013 | 0.027 | 0.06 |
| Velocity, m/s | 2829 | 3488 | 3562 | 3791 |
| Mach number | 5.9 | 5.3 | 5.3 | 5.4 |

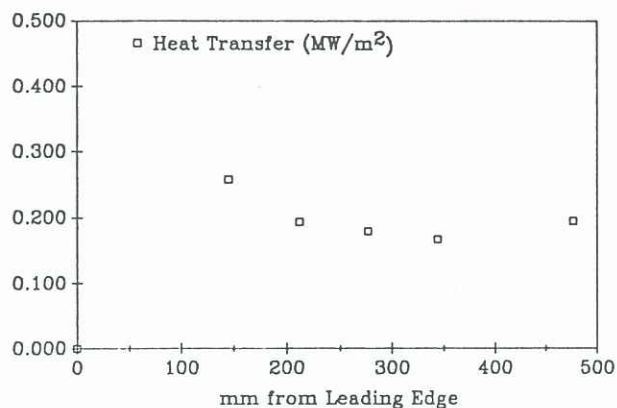


Figure 3 Heat transfer measurements (condition 1) used to calibrate skin friction gauges

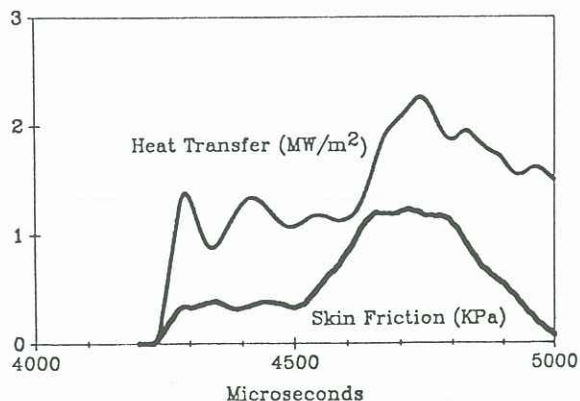


Figure 4 Skin friction and heat transfer time-histories at 145mm from leading edge for condition 2

It can be seen that the heat transfer trace and the skin friction trace follow each other. As noted however, in unsteady flow one lags the other as expected. It is therefore very important to calibrate one against the other only when conditions are steady and only in laminar flow (condition 1).

Figure 5 shows condition 2 at approximately 0.5 ms into the test time. Figure 6 shows condition 3. In both figures the rapid departure of skin friction and heat transfer distributions indicates the onset of transition. Figure 7 shows the theoretical prediction for shear stress from the heat transfer measurements and Reynolds analogy (open circles) for condition 2. The closed squares on this figure indicate the experimental shear stress measured in the flow.

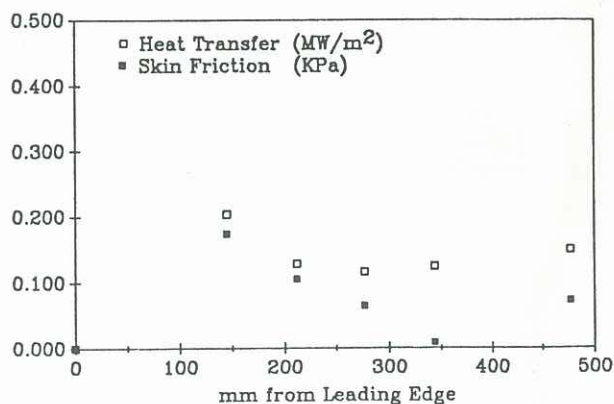


Figure 5 Heat transfer and skin friction along plate for condition 2

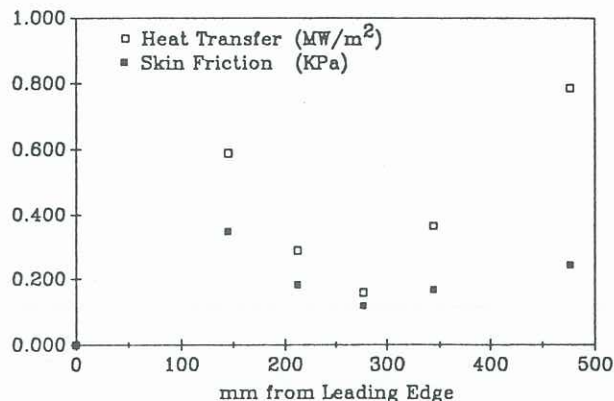


Figure 6 Heat transfer and skin friction along plate for condition 3

It can be seen from Figure 7 that when the flow is laminar (for the first three locations) agreement between theoretical predictions and experimental measurements is excellent. However, once the flow undergoes transition the measured values depart from theory. Although measurement and theory still follow the same trend, there is no longer a uniform scaling factor. For Figure 5 as well, it can be seen that when the flow is laminar, the skin friction and heat transfer results decay at similar rates and it is only once the flow undergoes transition that this pattern is disturbed. It must also be remembered that the heat transfer results tend to lag the skin friction

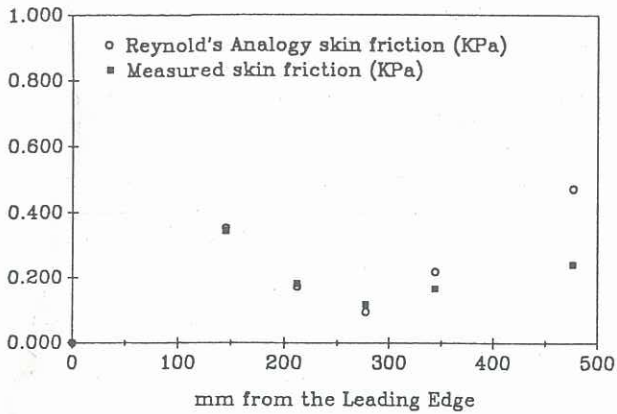


Figure 7 Measured and predicted skin friction along plate for condition 3

output. When change occurs, as in the onset of transition, this effect becomes noticeable.

Figure 8 shows results for condition 4. It appears that transition is occurring by the second gauge. The Reynolds number at gauge 2 is approximately 1.02×10^6 and the unit Reynolds number is $4.8 \times 10^6 \text{ m}^{-1}$. From results previously reported by He and Morgan (1989), it can be seen that for these values one would expect transition to occur somewhere between 200 and 260 mm from the leading edge. Gauge 2 is positioned at 210 mm from the leading edge.

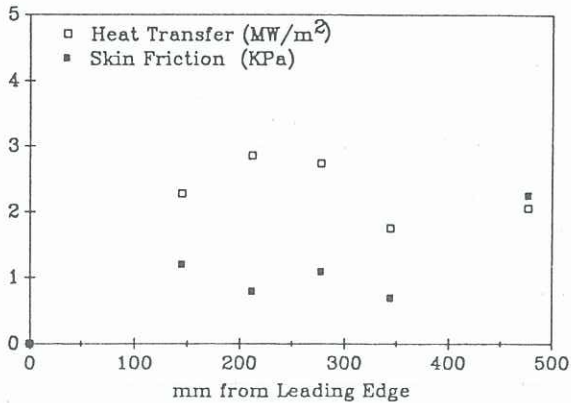


Figure 8 Heat transfer and skin friction along plate for condition 4

The discrepancy in Figure 8 between the skin friction and heat transfer trends at position two is a direct result of the lag between skin friction and heat transfer. It is evident though that the traces generally follow each other although only at the first point does Reynolds analogy hold. This once again is in agreement with the fact that Reynolds analogy is only purported to be held when conditions are laminar. It is interesting that during transition the general trend is still followed, although the factor between the two traces is no longer consistent.

CONCLUSIONS

It is concluded that where the flow is laminar, measurement of skin friction and heat transfer are consistent with Reynolds analogy. With the onset of transition Reynolds analogy, as expected, breaks down.

Also the skin friction gauge is shown to be an effective means of measuring shear stress. The gauge has a rise time of about $20 \mu\text{s}$, sufficiently short for most shock tunnel applications and approaching the rise times needed for expansion tube applications.

ACKNOWLEDGEMENTS

This work was supported by the Australian Research Council under Grant A5852080 and by NASA under Grant NAGW-674. The authors wish to acknowledge the invaluable technical contribution of John Brennan and the scholarship support from Zonta International Foundation.

REFERENCES

- DUNN, M G, (1981) Current Studies at Calspan Utilizing Short-Duration Flow Techniques. Proceedings of the 13th International Symposium on Shock Tubes and Waves, edited by C E Treanor and J G Hall, State Univ. of New York, Albany, NY, 32-40.
- HE, Y and MORGAN, R G, (1989) Transition of compressible high enthalpy boundary layer flow over a flat plate. 10th Australasian Fluid Mechanics Conference, Univ Melb, 11B-2, 11-15.
- KELLY, G M, SIMMONS, J M, and PAULL, A (1991) Skin-friction gauge for use in hypervelocity impulse facilities. AIAA Journal, 30, 844-845.
- VAN DRIEST, E R, (1952) Investigation of Laminar Boundary Layer in Compressible Fluids Using the Crocco Method. NACA TN 2597.